REFERENCES

[1] A. G. Williamson, "Equivalent circuit for radial-line/coaxial-line junction," *Electron. Lett.*, vol. 17, pp. 300–301, 1981.
[2] R. C. Allison, "A matched coaxial-radial transmission line junction," M.S. thesis, University of California, Los Angeles, 1977.
[3] R. C. Allison, R. L. Eisenhart, and P. T. Greiling, "A matched coaxial-radial transmission line junction," in *IEEE Int. Microwave Symp. Dig.*, 1978, pp. 44–46.
[4] A. G. Williamson, "Radial-line/coaxial-line junctions," University of Auckland, School of Engineering, Rep. no. 332, 1984.
[5] A. G. Williamson, "Radial-line/coaxial-line junctions—Analysis and equivalent circuits," to be published in the *Int. J. Electron.*
[6] P. I. Somlo, "The computation of coaxial line step capacitances," *IEEE Trans. Microwave Theory Tech.*, vol. MTT-15, pp. 48–53, 1967.
[7] D. C. Chang and T. T. Wu, "A note on the theory of end-corrections for thick monopoles," *Radio Sci.*, vol. 3 (new series), pp. 639–641, 1968.

New Analysis of Semiconductor Isolators : The Modified Spectral Domain Analysis

S. TEDJINI AND E. PIC

Abstract—**This paper addresses semiconductor isolators of the field displacement effect type. The semiconductor is modelized by its surface impedance tensor. This description allows an extension of the well-known spectral domain method to the analysis of the semiconductor isolators. Different configurations are studied and numerical results are given. The finline isolator with InSb is shown to be the best choice—indeed, insertion loss is less than 3 dB/cm and isolation is greater than 18 dB/cm. Experimental results supporting these calculations will be published in a following paper.**

I. INTRODUCTION

In view of the increasing use of the millimeter-wave band, one of the urgent problems of today is the development of nonreciprocal devices. The purpose of this paper is to describe some millimeter-wave semiconductor isolators using the field displacement effect.

The field displacement effect in gyroelectric structures at room temperature was demonstrated by Hirota and Suzuki [1]–[3] during 1969–1971 and is now well known.

The basic structure is a rectangular waveguide loaded in its E-plane by a thin slab of high-mobility semiconductor (such as InSb) which is transversally magnetized. The field displacement effect result from the superposition of TE_{m0} modes excited by the displacement current and the $TM_{m,n}$ modes excited by the conduction current on the semiconductor. The resulting electromagnetic field shows an asymetric distribution along the y-axis (see Fig. 1) which reverses with the direction of the wave propagation (or with the direction of the magnetostatic field).

This basic is a reciprocal one. In order to obtain some nonreciprocity, it is necessary to introduce a geometrical dissymmetry. Two nonreciprocal structures will be specially considered: the air-gap semiconductor loaded waveguide isolator, and the finline isolator.

Manuscript received March 2, 1984; revised July 9, 1984.

S. Tedjini is with the Laboratoire d'Electromagnétisme, Unité Associée au CNRS no. 833, ENSERG, 23 rue des Martyrs, 38031 Grenoble Cedex, France.
E. Pic is with the Laboratoire de Génie Physique, BP 46, Domaine Universitaire, 38402 St. Martin D'heres, Cedex, France.

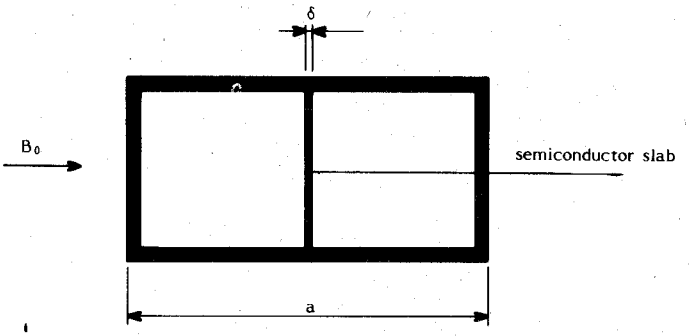

Fig. 1. Basic structure. In the E-plane of the waveguide we have a semiconductor slab submitted to magnetostatic field B_0. The semiconductor thickness is $\delta \ll a$.

A unified method will be presented to study the above structures. It is an extension of the well-known spectral domain technique (SDT) which takes into account the losses of the structure. It is then possible to compute the attenuation constant, and to derive the main parameters of the isolator: insertion losses and isolation.

In this paper (the first of two parts), the theoretical treatment is given with some details, together with computational results.

Experimental setups and results will be described in a second paper (to be published).

II. HISTORICAL REVIEW

There are two main classes of nonreciprocal semiconductor devices. In the first class, the semiconductor sample is longitudinally magnetized (the static magnetic field is parallel to the propagation direction). Such structures have been considered in [12], [13]. For instance, in [12], an InSb semiconductor at 77 K (mobility = 48 $m^2/V \cdot s$, conductivity = 1.5 10^3 s/m) with a length $l = 28.9$ mm exhibits a 2-dB insertion loss and a 30-dB isolation (frequency was 35 GHz and magnetic field 0.2 T). These results are very interesting. Unfortunately, the realization of such a device is difficult. Two drawbacks are low temperature operation (77 K) and longitudinal magnetization.

In the second class, the semiconductor slab is transversally magnetized. Operation at room temperature may be considered. This requires a very thin semiconductor plate to overcome the losses due to the semiconductor conductivity.

Several methods have been proposed to compute the propagation constant of a waveguide partially filled by a semiconductor and submitted to a magnetostatic field.

For instance, Gabriel and Brodwin [4] have used a perturbation method, where the nondisturbed field is the TE_{10} mode of the waveguide. The semiconductor introduces a perturbation operator: the field perturbation is projected on the basis of the eigenmodes of the waveguide. However, this method is not valid for a strong perturbation, namely for a high semiconductor conductivity.

Hirota and Suzuki [2] used a variational method assuming a lossless semiconductor. This method determines the phase constant and exhibits the field displacement effect. But their calculation did not take into account the dielectric substrate.

Another pertinent treatment is the Schelkunoff method [6]. This method has been used by Arnold and Rosenbaum [7], and by J. L. Amalric [8] in the case of anisotropic inhomogeneous waveguide. This last author gave an interesting discussion of the advantages and drawbacks of this method.

0018-9480/85/0100-0059$01.00 ©1984 IEEE

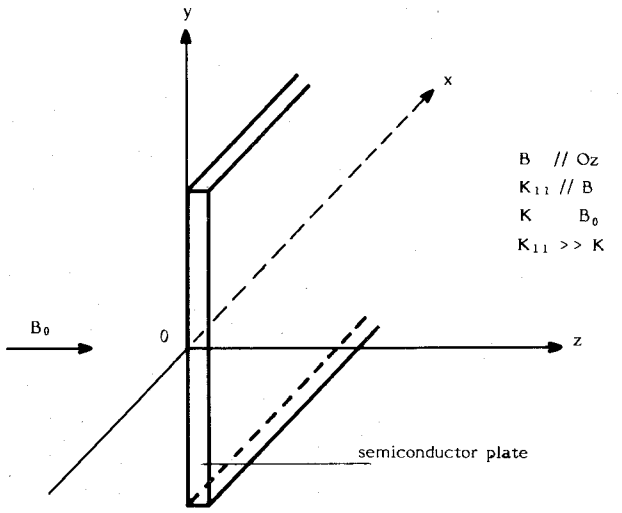

Fig. 2. Semi-infinite semiconductor plate submitted to a x-directed magnetostatic field B_0.

The major advantage of the latter method is its ability to study a more general case: a semiconductor slab on a dielectric substrate anywhere in the waveguide.

The Schelkunoff's method shows two disadvantages. First, it is not well suited for high-conductivity materials inside the waveguide and can't be considered in the case of a finline isolator. Second, there is a problem with the choice of the modes used in the projection of the solution on the waveguide eigenmodes. Different selection criteria may be considered. The most important criterion is the values of coupling impedances between the eigenmodes. The numerical solution depends on the choice of eigenmodes.

The SDT is a powerful tool for analyzing planar microwave structures. We shall show in this paper how it can be used to calculate the pertinent parameters of a semiconductor isolator by taking into account the losses of the semiconductor slab. In this method, the semiconductor is described by its impedance (or conductivity tensor). The SDT seems well suited for high-mobility or conductivity semiconductors.

III. Modelization of the Semiconductor Layer

The wave in a semi-infinite high-conductivity semiconductor, which is submitted to the magnetostatic field perpendicular to the interface, is easily shown to propagate almost along the magnetic field B_0 mathematically: $k_{11} \ll k\perp, k_{11}$ is the propagation constant parallel to B_0 and $k\perp$ is the one perpendicular to B_0.

These are two quasi-circular waves. The transverse components are circularly polarized and the longitudinal ones are quite negligible. The two propagation constants are the helicon and the antihelicon ones.

If one considers a plate of thickness δ, the electromagnetic field is even or odd. For an even mode, the transverse electric field is maximum at the center of the plate, e.g., the impedance in this plane is an open circuit. By the transmission-line theory, one obtains the surface impedances for the two quasi-circular modes in the usual rotating frame (see Fig. 2). Returning to the Cartesian components of the field, we get a surface impedance tensor defined by the following relation:

$$\vec{E}_T = Z_s \cdot \vec{H}_T. \tag{1}$$

E_T and H_T are the tangential electric and magnetic field on the semiconductor. Z_s is a 2×2 matrix. Its elements are function of the semiconductor characteristics.

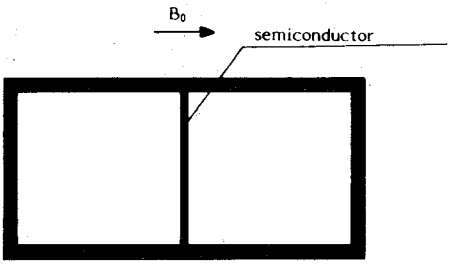

Fig. 3. Basic structure studied by Hirota and Suzuki.

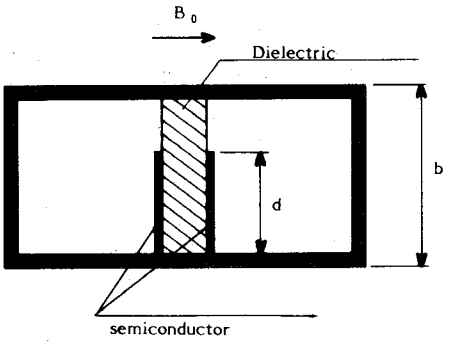

Fig. 4. Air-gap semiconductor isolator $d < b$.

When the thickness of the plate δ is small compared to the wavelength in the semiconductor, the expression of Z_s is simplified. So, by considering the current density instead of the RF magnetic field, one ends at the following relation between the tangential electric field E_T and the current density J_T on the semiconductor layer:

$$\vec{J}_T = \delta\sigma\vec{E}_T \tag{2}$$

where δ is the thickness of the semiconductor and σ is the conductivity tensor given by

$$\sigma = \begin{vmatrix} \sigma_\perp & \sigma_x \\ \sigma_x & \sigma_\perp \end{vmatrix}$$

$$\sigma = \sigma_0 \frac{1 + j\omega\tau}{(1+j\omega\tau)^2 + \omega_c^2\tau^2} \qquad \sigma = \sigma_0 \frac{\omega_c\tau}{(1+j\omega\tau)^2 + \omega_c^2\tau^2} \tag{3}$$

σ_0 semiconductor conductivity,
$\omega_c = eB/m^*$ cyclotron frequency,
e and m^* electron charge and the effective mass, respectively,
ν $= 1/\tau =$ collision frequency,
B_0 = magnetostatic field perpendicular to the semiconductor.

IV. Theoretical Analysis

Figs. 3–5 show different structures.

The most general case is the finline isolator (Fig. 5). Structures given in Figs. 3 and 4 may be studied by using the Schelkunoff's method. Because of the presence of the fins (infinite conductivity) in Fig. 5, the former method can't be used, so we propose an extension of the SDT.

Fig. 6 shows the pertinent dimensions in the general case. This structure is a bilateral finline with two semiconductor layers in the planes $x = \pm c/2$. A magnetostatic field is x-directed.

We solve for even modes which see a magnetic wall in the plane of symmetry $x = 0$. The electromagnetic field in each region, dielectric and air, is expressed as a superposition of the LSE and LSM modes. The pertinent Hertz potentials are x-

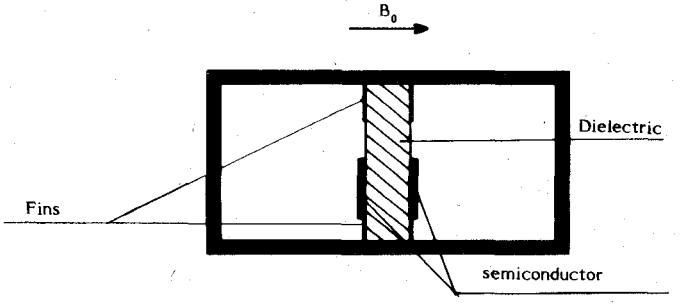

Fig. 5. The most general case. The finline isolator.

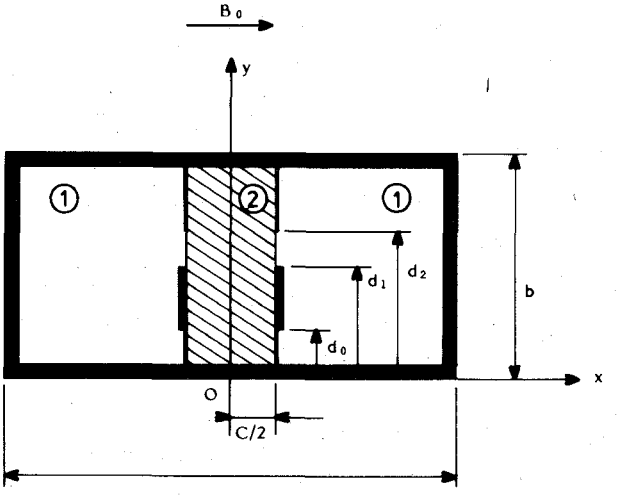

Fig. 6. The studied structure. It is a bilateral finline loaded by a semiconductor slab. The semiconductor lies between $y = d_0$ and $y = d_1$. The media 1 is the air and the media 2 is a dielectric ($\epsilon_2 = \epsilon_0\epsilon_r$).

directed

$$\vec{\Pi}(x,y,z,t) = \phi(x,y)\cdot\exp[\,j(\omega\tau - \beta z)]\,\bar{x} \tag{4}$$

where β is the propagation constant (phase constant and attenuation) and ω is the angular frequency. The function $\phi(x,y)$ is developed in the Fourier series along the direction.

Let E_y and E_z be the tangential components of electric field in the slot (between the two fins in the plane $x = c/2$). Applying the continuity conditions at $x = c/2$, one obtains a fundamental relation between the Fourier coefficients of the current density and the Fourier coefficients of the tangential electric field. This relation reads

$$\vec{J}_n = M_n \cdot \vec{E}_n. \tag{5}$$

M_n is a 2×2 matrix. Its elements are known functions of the structure dimensions a, b, c, the frequency, and the dielectric constant.

The relation (5) is a classical one and may be found in other works in connection with the finline [9]–[11] and (or) the microstripline.

Now, we shall introduce the semiconductor in the equations. The relation (5) is equivalent in ordinary space to

$$\vec{\mathscr{J}}_s(y) = \mathscr{M}\vec{\mathscr{E}}(y) \tag{6}$$

where $\mathscr{M}$ is a known operator independent from the semiconductor parameters. The current $\vec{\mathscr{J}}_s(y)$ has tow components: current on the fins $\vec{\mathscr{J}}_f(y)$, and current on the semiconductor $\vec{\mathscr{J}}_{sc}(y)$. Then

$$\vec{\mathscr{J}}_s(y) = \vec{\mathscr{J}}_f(y) + \vec{\mathscr{J}}_{sc}(y). \tag{7}$$

Previously, we expressed the following boundary conditions on the semiconductor (2), which we write again as

$$\vec{\mathscr{J}}_{sc}(y) = \delta\sigma\cdot\mathscr{E}(y) \tag{8}$$

where δ is the thickness of the semiconductor and σ its conductivity. Thus, the new fundamental relation between the fin current and the slot field is

$$\vec{\mathscr{J}}_f(y) = (\mathscr{M} - \delta\sigma)\mathscr{E}(y). \tag{9}$$

If the semiconductor thickness goes to zero in (9) (no semiconductor), we get the classical finline case (relation (6)).

To solve (9), the analysis goes on as in [9 eq. (10)]. One notes that all quantities are complex. Let us write the following slot-field expressions:

$$\mathscr{E}_y(y) = \sum_i a_i f_i(y)$$
$$\mathscr{E}_z(z) = \sum_i b_i g_i(y) \tag{10}$$

where $f_i(y)$ and $g_i(y)$ are known basic functions and a_i, b_i are unknown complex coefficients.

The expression (10) is valid in the slot, namely for $d_0 < y < d_2$. On the fins $0 < y < d_0$ and $d_2 < y < b$, the electrical field is zero.

Since the electrical field and fin current are defined in complementary domains

$$\begin{array}{llll} \mathscr{J}_f \neq 0 & 0 \leqslant y \leqslant d_0 & d_2 \leqslant y \leqslant b & \vec{\mathscr{E}}_T = 0 \\ \mathscr{J}_f = 0 & d_0 \leqslant y \leqslant d_2 & \vec{\mathscr{E}}_T \neq 0 & \end{array}$$

then the two relations are verified

$$\frac{1}{b}\int_0^b \mathscr{J}_{fy}(y)\cdot f_i(y)\,dy = 0, \quad \frac{1}{b}\int_0^b \mathscr{J}_{fz}(y)\cdot g_i(y)\,dy = 0. \tag{11}$$

Equation (11) gives a system of linear equations. The unknowns are the coefficients a_i, b_i. The determinant of the system (11) is a transcendental function of frequency and propagation constant. The zeroing of the determinant gives the propagation constant and then the field and power distribution.

The detailed form of the determinant and the procedure for the search of the solutions of the determinantal equation may be found in [11].

The computation is achieved with trigonometric basis functions. In all cases, the relative convergence criterion is satisfied and one needs typically five basis functions. In this case, the computation time is about 5 s on a HB 68-CII Multics Computer.

V. Computation Results

Two semiconductors have been considered: 1) InSb because of its high mobility, and 2) GaAs because it is an interesting media for millimeter-wave integrated circuits (MIC's).

From the calculation, one gets the complex propagation constant: phase constant and attenuation constant.

A typical variation of the phase constant β is given in Fig. 7.

The forward phase constant β^+ and the backward one β^- are plotted versus the semiconductor fin height. One notices a differential phase shift. Such an effect could lead to the realization of a nonreciprocal phase-shift device. But this requires very low insertion losses.

In the next sections, only the attenuation constants (α^+ for the forward propagation and α^- for the backward propagation) will be further discussed. The insertion losses are defined by

$$L(\mathrm{dB/cm}) = 20\log_{10}\left[\exp\left(\frac{\alpha^+}{100}\right)\right] = 8.68\ 10^{-2}\alpha^+.$$

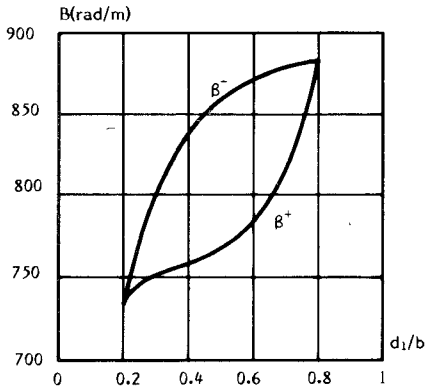

Fig. 7. A typical variation of β^+ and β^- versus the semiconductor height. The InSb thickness is 2×1 μm. Finline case $d_0 = 0.2b$, $d_2 = 0.8b$, $f = 36$ GHz, $B_0 = 0.8T$, $c = 0.125$ mm, $\epsilon_r = 5.5$.

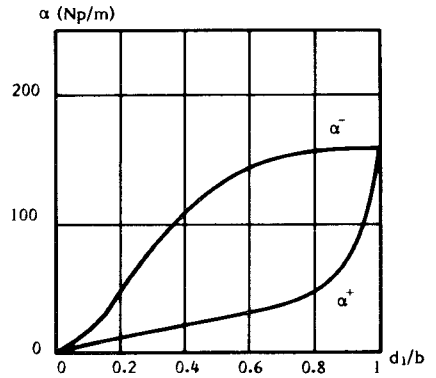

Fig. 8. Forward α^+ and backward α^- attenuations versus the semiconductor height. The InSb thickness is 2×1 μm. Air-gap isolator $d_0 = 0$, $d_2 = b$, $f = 36$ GHz, $B_0 = 0.8T$, $c = 0.125$ mm, $\epsilon_r = 5.5$.

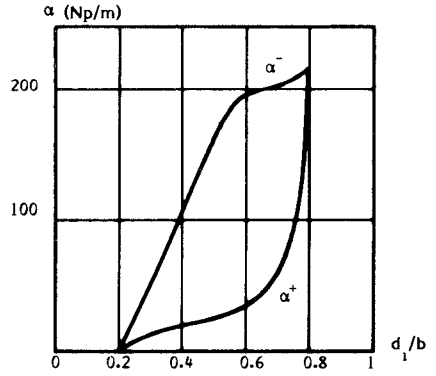

Fig. 9. Forward α^+ and backward α^- attenuations versus the semiconductor height. The InSb thickness is 2×1 μm. Finline isolator $d_0 = 0.2b$, $d_2 = 0.8b$, $f = 36$ GHz, $B_0 = 0.8T$, $c = 0.125$ mm, $\epsilon_r = 5.5$.

The isolation is given by

$$I(\text{dB/cm}) = 20\log_{10}\left[\exp\left(\frac{\alpha^-}{100}\right)\right] = 8.68\ 10^{-2}\alpha^-.$$

A. Effect of Semiconductor Fin

Figs. 8–11 give the variation of the attenuation constants (α^+ and α^-) versus the semiconductor fin height.

Figs. 8 and 9 are relative to a 1-μm thickness of GaAs. In all cases, the dielectric substrate is 0.125 mm, frequency is 36 GHz, and the magnetic field 0.8 T.

Let us consider first InSb (Fig. 7). The conductivity of the semiconductor is $\sigma = 1.7\ 10^4$ S/m and the low-field electronic mobility is $\mu = 6$ m^2/V·s. The permittivity of the dielectric is 5.5.

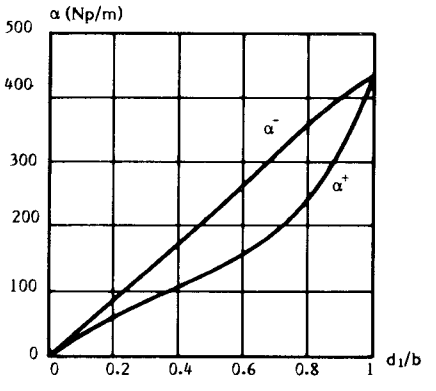

Fig. 10. Forward α^+ and backward α^- attenuations versus the semiconductor height. The GaAs thickness is 2×1 μm. Air-gap isolator $d_0 = 0$, $d_2 = b$, $f = 36$ GHz, $B_0 = 0.8T$, $c = 0.125$ mm.

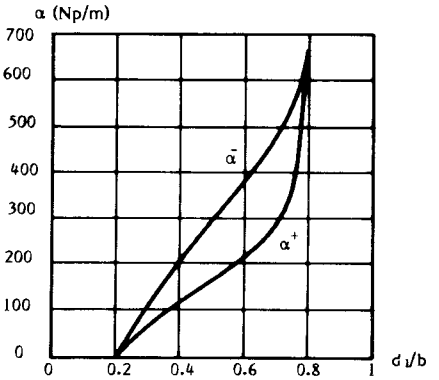

Fig. 11 Forward α^+ and backward α^- attenuations versus the semiconductor height. The GaAs thickness is 2×1 μm. Finline isolator $d_0 = 0.2b$, $d_2 = 0.8b$, $f = 36$ GHz, $B_0 = 0.8T$, $c = 0.125$ mm, $\epsilon_r = 12$.

One notes a 2-dB/cm insertion loss and 9-dB/cm isolation for a normalized height $d/b = 0.6$. The performances of the isolator are greatly enhanced by the use of finline technology (Fig. 9). This improvement arises since the fins concentrate the power near the conductor edges. One notices an important improvement of the isolation (>17 dB/cm) at the expense of increasing the insertion losses up to 2.9 dB/cm.

We have carried out the same computations with GaAs, the conductivity $\sigma = 3000$ S/m and the low electronic mobility $\mu = 0.5$ m/V·s. The results are shown in Figs. 10 and 11. In all cases, the performances degrade with the substitution of GaAs to InSb. The insertion losses ($d/b \simeq 0.6$) are very high (>10 dB/cm).

A comparison between the previous cases is given Table I. In conclusion, it is necessary to verify the condition $\mu B_0 > 1$. The higher the product μB_0, the higher the isolation, and the smaller the insertion losses. One concludes that GaAs is not interesting for this application. Hence, only InSb will be considered in the next computations.

B. Effect of Slot Width

Fig. 12 gives the variation of α^+ and α^- versus the slot width. The other parameters are given in the figure. The slot width $d/b = 0.6$ seems a possible optimum (which is given by the maximum of $\dfrac{\alpha^- - \alpha^+}{\alpha^+}$. In this case, we have $\alpha^+ = 28$ Np/m and $\alpha^- = 158$ Np/m.

TABLE I
COMPARISON BETWEEN INSB AND GAAS

Semiconductor	Slot width	d_0/b	d_1/b	d_2/b	α^+ Np/m	α^- Np/m	Losses dB/cm	Isolation dB/cm
InSb, $\delta = 2\times1\ \mu$m	b	0	0.6	1	25	115	2.1	1.0
InSb, $\delta = 2\times1\ \mu$m	$0.6b$	0.2	0.6	0.8	35	195	2.9	16.9
GaAs, $\delta = 2\times1\ \mu$m	b	0	0.6	1	155	260	13.5	22.6
GaAs, $\delta = 2\times1\ \mu$m	$0.6b$	0.2	0.8	0.8	220	400	19.1	34.7

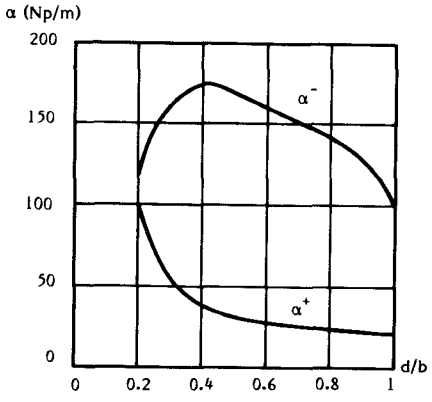

Fig. 12. Forward α^+ and backward α^- attenuations versus the slot width $d/b = (d_2 - d_0)/b$. The InSb lies between d_0 and $d_1 = 0.5b$, $f = 36$ GHz, $B_0 = 0.8T$, $c = 0.125$ mm, $\epsilon_r = 5.5$.

C. Broad-Band Operation

Fig. 13 gives the behavior of attenuation constants α^+ and α^- in the case of the InSb slab, when the frequency is swept between 30 and 40 GHz (*Ka*-band). One notices that α^+ is quasi-independent from frequency, but α^- increases linearly from 220 N_p/m to 280 N_p/m. One concludes that the device may be operated in quite a broad band.

D. Field Displacement Effect

To illustrate the field displacement effect, we have drawn the power distribution in the cross section of the line for two propagation directions.

Fig. 14(a) is relative to the forward propagation. The power is concentrated on the slot near the edge of the fin leading to a small attenuation.

Fig. 14(b) is relative to the backward propagation. The power is concentrated on the semiconductor where the attenuation is high.

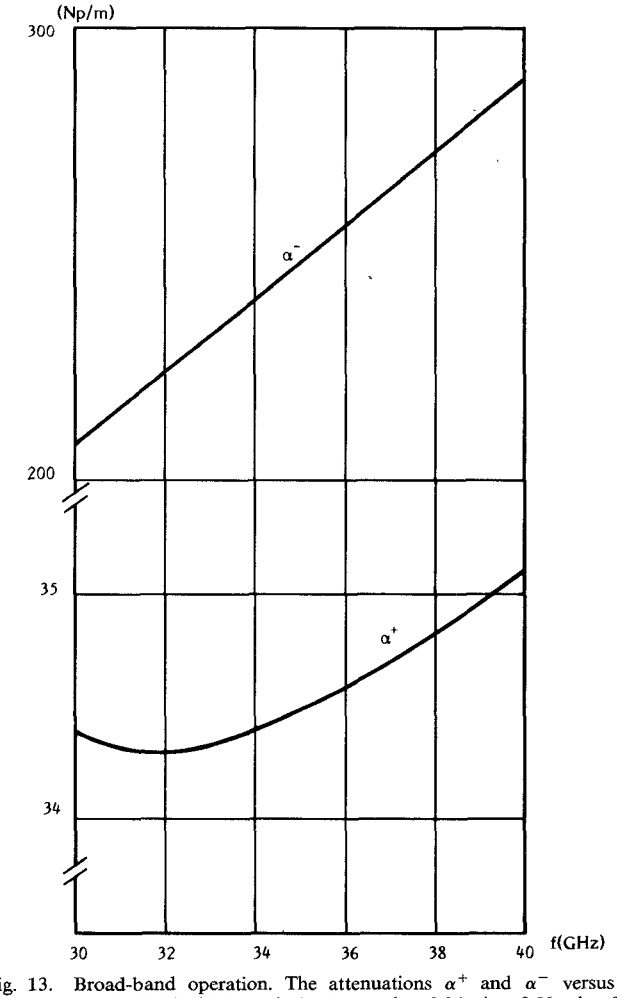

Fig. 13. Broad-band operation. The attenuations α^+ and α^- versus the frequency. The InSb thickness is $2\times1\ \mu$m. $d_0 = 0.2b$, $d_2 = 0.8b$, $d_1 = 0.6b$, $B_0 = 0.8T$, $c = 0.125$ mm, $\epsilon_r = 5.5$.

VI. CONCLUSION

We describe in this paper a new theoretical computation of the field displacement effect–semiconductor isolator. It relies on two main ideas.

First: the modellization of a high-conductivity semiconductor slab by a surface impedance tensor. This allows an easy expression of the boundary conditions.

Second: the S.D.T. is adapted to take into account the presence of lossy surface impedance. This approach has allowed us to compute insertion losses and the isolation per unit length of an infinite isolator structure.

A comparison between InSb and GaAs is done. InSb appears to be the best choice at room temperature and for reasonable values of the static magnetic field. Calculations show the large enhancement of the isolation when using the finline technology.

Experimental results (to be published) for the AsGa agree within 10 percent with the computed prediction.

REFERENCES

[1] K. Suzuki, "Room temperature solid state plasma non reciprocal microwave devices," *IEEE Trans, Electron Devices*, vol. ED-16, pp. 1018–1021, 1969.

[2] R. Hirota and K. Suzuki, "Field distribution in a magneto-plasma loaded waveguide at room temperature," *IEEE Trans. Microwave Theory Tech.*, vol. MTT-18, pp. 188–195, Apr. 1970.

[3] K. Suzuki and R. Hirota, "Nonreciprocal millimeter wave devices using a soldid state plasma at room temperature," *IEEE Trans. Electron Devices*, vol. ED-18, pp. 408–411, July 1969.

[4] G. J. Gabriel and M. E. Brodwin, "Perturbation analysis of rectangular waveguide containing transversely magnetized semiconductor," *IEEE Trans. Microwave Theory Tech.*, vol MTT-14, pp. 258–264, June 1966.

[5] E. Pic and B. H. Luong, "Galerkin method calculation of the propagation constant in a gyroelectric inhomogeneous waveguide," *Proc. 8th Eur. Microwave Conf.* (Paris), 1978, pp. 236–140.

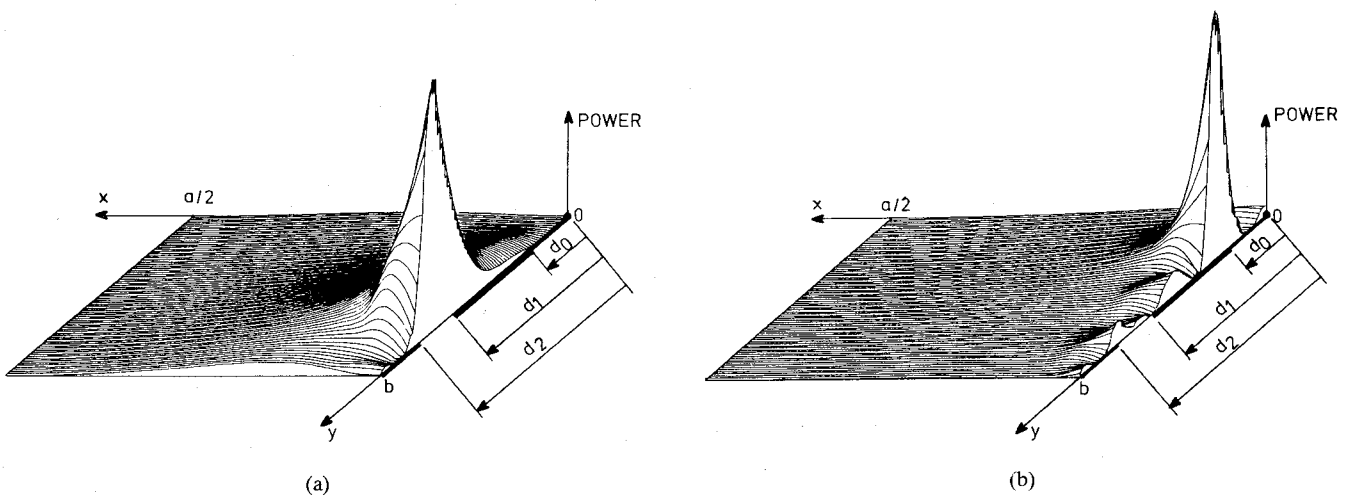

Fig. 14. Power density on the half cross section of finline. The power is concentrated on the slot. The InSb thickness is 2×1 μm, finline isolator $d_0 = 0.2b$, $d_2 = 0.8b$, $f = 36$ GHz, $B_0 = 0.8T$. This is the forward case. (b) Power density on the half cross section of finline. The power is concentrated on the semiconductor. The parameters are given in Fig. 14(a). This is the backward case.

[6] S. A. Schelkunoff, "Generalized telegraphist's equations for waveguides," *Bell Syst. Tech. J.*, vol. J.31, pp. 784–801, July 1982.
[7] R. M. Arnold and F. J. Rosenbaum, "Nonreciprocal wave propagation in semiconductor loaded waveguides in the presence of a transverse magnetic field," *IEEE Trans. Microwave Theory Tech.*, vol. MTT-19, pp. 57–65, Jan. 1971.
[8] J. L. Amalric, "Contribution à l'étude de l'effet de déplacement de champ dans les guides chargés par les lames semiconductrices," thèse de doctorat d'etat INP Toulouse, France, 1978.
[9] H. Hofmann, "Dispersion of planar waveguides for millimeter wave application," *Arch. Elek. Übertragung*, vol. 31, pp. 40–44, Jan. 1977.
[10] E. Pic, S. Tedjini, and C. Nasrallah, "Une nouvelle ligne integrable millimétrique: la finline," *Annales des Télécommunications*, vol. 37, no. 11–12, pp. 461–476, 1982.
[11] S. Tedjini, "Contribution à l'étude d'un isolateur à semiconducteur pour ondes millimétriques: application à la fin-line," doctorat thesis, INP Grenoble, France, 1982.
[12] B. R. MacLeod and W. G. Way. "A 35-GHz isolator using a coaxial solid state in a longitudinal magnetic field," *IEEE Trans. Microwave Theory Tech.*, vol. MTT-19, pp. 510–516, June 1971.
[13] M. Kanda and W. G. May, "Hollow-cylinder waveguide isolators for use at millimeter wavelengths," *IEEE Trans. Microwave Theory Tech.*, vol. MTT-22, pp. 913–917, Nov. 1974.

Biological Tissues Characterization at Microwave Frequencies

B. D. KAROLKAR, J. BEHARI, AND A. PRIM

***Abstract*—The present work is concerned with the measurement of dielectric permittivity and conductivity of various high loss tissues from freshly sacrificed animals. The measurement makes use of the 'infinite sample' technique which involves mounting of the sample in a rectangular waveguide system excited in the TE_{10} mode at 9.4 GHz. A more complex system consisting of skin-fat-muscle combination is also studied. An evaluation of relaxation times is made in all the cases. It is hoped that these data will be relevant in further quantifying the available results in this frequency range.**

Manuscript received February 8, 1984; revised July 9, 1984. This work was supported in part by ICMR, India.

The authors are with the School of Environmental Sciences, Jawaharlal Nehru University, New Delhi-110 067, India.

I. Introduction

Biological effects of microwave radiation have been the focus of various research efforts in the last decade. Key to this is the determination of the complex permittivity (ϵ' and ϵ'') of biological tissues. Although *in vivo* methods have been attempted in the recent past [1], no data are available on dielectric measurements of tissues like stomach, intestine, and heart in the gigahertz frequency range, though some measurements for kidney and liver have been recently reported [2]. In an effort to bridge this gap, a detailed survey has been undertaken of almost all the available biological tissues. The chosen method would have to be one which could be uniformly adopted for all such tissues and at the same time be fairly quick and simple. This would allow measurements on fresh tissues, thus ensuring essential sample configuration. Dictated by these factors, the 'infinite sample' technique was adopted for the measurement of dielectric parameters of high-loss tissues at microwave frequencies.

In order to compare our measurements with those of other techniques [2], we have included some of the tissues like muscle, spleen, and liver, and also the muscle phantom tissue for which fairly reliable data are available [3]. Besides these, tissues like intestine, stomach, spleen, heart, and a more complex system consisting of a skin, fat, and muscle combination were also studied. The measurements were performed at 9.4 GHz. The frequency was chosen to be in the gigahertz range in view of the possibility of the use of high-frequency electrical energy as an effective method of selectively heating local masses of tissues, while the surface heating of tumors has also been proposed [4].

II. Theoretical Background of the 'Infinite Sample' Technique [5]

When a physically reasonable length of the sample dissipates a sufficiently large portion of the microwave energy entering the sample so that no energy is reflected to the input terminal, the sample may be considered to be of 'infinite length'. Thus, making use of the 'infinite sample' technique, the measurement requires the determination of essentially only the normalized input impedance at the sample face. The dielectric permittivity and the loss

0018-9480/85/0100-0064$01.00 ©1984 IEEE